

**International Journal of Biomedical Research**

ISSN: 0976-9633 (Online); 2455-0566 (Print)

Journal DOI: <https://doi.org/10.7439/ijbr>

CODEN: IJBRFA

Original Research Article

**Evaluation of selective laser sintered polyamide/hydroxyapatite composite compositions –*in vitro* and *in vivo*****Banu Pradheepa Kamarajan<sup>1</sup>, Ramu Murugan<sup>2</sup>, Ananthasubramanian Muthusamy<sup>1\*</sup>,  
Dinakar Rai B K<sup>3</sup>, Vignesh Mathialagan<sup>3</sup> and Shanthakumari S<sup>4</sup>**<sup>1</sup>Department of Biotechnology, PSG College of Technology, Coimbatore, India<sup>2</sup>Department of Mechanical Engineering, PSG College of Technology, Coimbatore, India<sup>3</sup>Department of Orthopedics, PSG Institute of Medical Sciences & Research, Coimbatore, India<sup>4</sup>Department of Pathology, PSG Institute of Medical Sciences & Research, Coimbatore, India

QR Code

**\*Correspondence Info:**Dr M. Ananthasubramanian,  
Professor & Head,  
Department of Biotechnology,  
PSG College of Technology, Coimbatore – 641 004, Tamil Nadu, India**\*Article History:****Received:** 02/08/2017**Revised:** 24/08/2017**Accepted:** 24/08/2017**DOI:** <https://doi.org/10.7439/ijbr.v8i8.4322>**Abstract****Objective:** To study the suitability of the developed polyamide/hydroxyapatite (PA/HA) composite orthopaedic scaffold in *in vitro* and *in vivo*.**Methods:** The fabricated scaffolds were seeded with human osteoblast-like cell line (MG 63) and tested for its viability & cytotoxicity, proliferation and calcium mineralization through MTT assay, ALP assay and Alizarin red S staining respectively. Finally, the scaffolds were implanted in non-immunocompromised male wistar rats subcutaneously and pathological tests were carried out.**Results:** The results of *in vitro* studies indicate that PA/HA (90:10) composite was non-cytotoxic and supported calcium mineralization relatively better than the other compositions of PA/HA. From the Hematoxylin & Eosin staining, inflammation was observed in the tissues surrounding the scaffold 7 weeks post implantation in rats. However, the scaffolds were found to be incorporated into the subcutaneous tissue at the end of one year without any rejection.**Conclusion:** PA/HA (90:10) composite scaffold fabricated using SLS is biocompatible when tested in rats, and could more likely be used for orthopedic applications.**Keywords:** Scaffold, orthopedic, biocompatibility, MG 63, rat model.**1. Introduction**

Recent reports suggest that among the total injuries due to accidents, 11.5% are bone fractures [18]. Besides fractures, bone replacement is also essential for patients with congenital disorders, tumor resection, and those in a revision surgery to replace the infected implant. This signifies the need for a material that is mechanically strong and biologically compatible to be a good orthopedic scaffold.

Pure HA is a bioactive ceramic known for its osteoinductive property. However, its brittle nature makes it unsuitable to repair the bone defect by itself. Hence, HA is used along with PA. This polymer/ceramic composite yields greater strength [14].

PA and HA are being used as bone scaffolds for many years. Conventional techniques such as freeze-drying and cross-linking [15], thermally induced phase separation [16] and injection-molding technique [17] were used to develop PA/HA scaffolds.

However, Selective laser sintering, a rapid prototyping technique helps in customized development of 3D porous PA/HA composite scaffolds with 100% pore interconnectivity. Here we present the *in vitro* and *in vivo* performance of the 3D porous scaffold of different compositions of PA and HA fabricated using SLS.

PA 66 was used by many researchers [7,8,11,14] for developing the bone scaffold. But in this study, PA 12 is employed. Though PA12 is cost ineffective compared to

PA66, it has the advantage of resistance to corrosion, cracking and chemical degradation [19, 20].

PA/HA scaffolds fabricated using Selective Laser Sintering, an additive manufacturing technique described elsewhere [5] is used in this study.

The aim of this work is to analyze the *in vitro* and *in vivo* performance of the 3D porous scaffold fabricated with different compositions of PA and HA fabricated using SLS, for its use as an orthopedic scaffold.

## 2. Methods

### 2.1. Polyamide/hydroxyapatite scaffold

PA 12 was purchased from Duraform 3D systems, and HA was synthesized chemically as per the protocol specified by Sneha *et al* [9]. PA and PA/HA composite scaffolds were fabricated in Selective Laser Sintering machine (Sinterstation DTM 2500 *plus*). The scaffolds have cubical pores of size 800  $\mu\text{m}$  contributing for 70% porosity. 3D porous scaffolds of cubical shape (0.9 x 0.9 x 0.4 cu.mm.) and cylindrical shape (0.9 mm diameter and 0.4 mm thickness) were used for *in vitro* and *in vivo* studies respectively. The images of the fabricated scaffolds are presented in Figure 1.

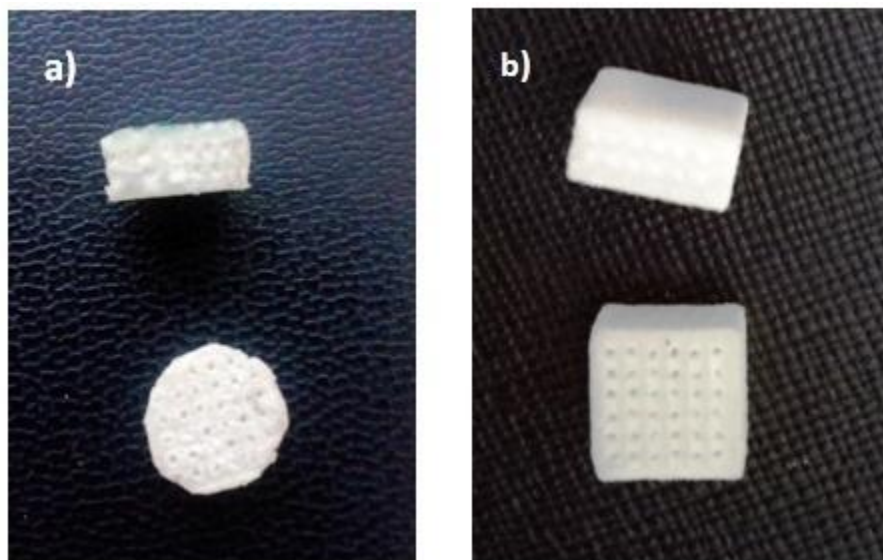


**Figure 1: Three dimensional porous scaffolds a) cylindrical shape with 0.9 mm diameter and 0.4 mm height used for *in vivo* testing; b) cubical shape with dimensions 0.9x0.9x0.4 cu.mm used for *in vitro* testing**

### 2.2. Cell culture

The human osteosarcoma cell line, MG-63, (NCCS Pune, India) was cultured in DMEM medium (AL007S, HiMedia, India) supplemented with 200mM L-glutamine, 10% Fetal bovine serum, and 1X of Antibiotic Antimycotic Solution (A002, Himedia, India). The cells were incubated with 5% CO<sub>2</sub> at 37°C. On attaining 80-90% confluency, the cells were trypsinized with trypsin-EDTA. Unless specified, the chemicals were procured from HiMedia, India.

### 2.3. Cell viability and proliferation studies

MTT assay was employed to assess the cell viability and proliferation of the cells on interacting with the scaffold material. This is a colorimetric assay measuring the reduction of yellow 3-(4, 5-dimethylthiazol-2-yl)-2, 5-diphenyl tetrazolium bromide (MTT) substrate to an insoluble purple formazan product by mitochondrial succinate dehydrogenase enzyme. The MTT enters the cells and passes into the mitochondria where it gets reduced to an insoluble, dark purple colored formazan product. The

intensity of the purple color is proportional to the number of live cells.

Each well containing the UV sterilized scaffold was seeded with 1000  $\mu\text{L}$  of medium containing approximately  $1 \times 10^4$  cells. The plates were incubated at 37°C with 5% CO<sub>2</sub>. MG 63 cells cultured without any scaffold was used as the control. After 1, 3 and 5 days of incubation, 5mg per ml of freshly prepared MTT (HiMedia, India) solution was added to each well and incubated for 3.5 h at 37°C with 5% CO<sub>2</sub>. After the incubation time, the above solution was discarded and the scaffolds were air dried. The insoluble purple colored formazan crystals formed were solubilized by adding 200  $\mu\text{l}$  of Dimethyl sulphoxide (SD Fine Chemicals). The plate was left in shaking condition for 10-15 min in dark. The solutions from 48-well plate were then transferred to 96-well plate and, the absorbance was read at 570 nm in a multiwell plate reader (Thermo Multiscan Labsystems, Model 352). The absorbance values were plotted in graph using MS Excel.

#### 2.4. Alkaline Phosphatase assay

Alkaline phosphatase (ALP) is a hydrolase enzyme responsible for removing phosphate groups from nucleotides, proteins, and alkaloids. Higher levels of ALP activity is observed during the active bone formation, as it is a by-product of the osteoblast activity and, also observed in elevated levels in the cell membrane of undifferentiated pluripotent cells. The alkaline phosphatase assay was carried out using the p-nitrophenol pyrophosphate (N7653 Sigma Aldrich) as the substrate according to the protocol specified by the manufacturer. ALP catalyses the hydrolysis of the colorless p-Nitrophenyl phosphate (pNPP) to a colored p-Nitrophenol, that has a strong absorbance at 407 nm. The absorbance is a measure of the level of the enzyme activity.

Each well containing a UV sterilized scaffold was seeded with 1000 µL of medium containing approximately  $1 \times 10^4$  cells in a 48 well plate, and incubated for 4, 7 and 10 days at 37°C with 5% CO<sub>2</sub>. After the incubation, 200µL of p-nitrophenol pyrophosphate solution was added to each well. The plates were then incubated in dark for 30 minutes at room temperature. After 30 minutes, 50µL of 3M NaOH solution was added per 200 µL of the reaction mixture to stop the reaction. The absorbance was then read at 407 nm in a multiwell plate reader (Thermo Multiscan Labsystems, Model 352). Statistical analyses for MTT and ALP assays were carried out using paired t-test using MINITAB 15.0 software. P<0.005 were considered to be statistically significant.

#### 2.5. Alizarin Red S staining

Alizarin Red S, an anthraquinone derivative, is used to identify calcium in tissue sections. The reaction is not strictly specific for calcium, since magnesium, manganese, barium, strontium, and iron may interfere. But as these elements usually do not occur in sufficient concentration in this experiment to interfere, the scaffolds were tested for calcium mineralization using Alizarin red S staining. Alizarin Red S powder (A5533 Sigma Aldrich) was used to prepare a fresh solution (pH 4.1-4.2) each time as per the protocol specified by Gregory *et al*, 2004 [3].

Each well containing a UV sterilized scaffold was seeded with 1000 µL of medium containing approximately  $1 \times 10^4$  cells in a 48 well plate, and was incubated for 25 and 28 days at 37°C with 5% CO<sub>2</sub>. After the incubation period, the media was discarded, and the wells were rinsed gently with 1 mL PBS. The cells were then fixed with 1.0 mL of 10% formalin in each well for 15 minutes at room

temperature. Formalin solution was then removed and the wells were washed twice gently with double distilled water. To each well, 500 µL of 40 mM Alizarin red S solution was added and left at room temperature for 20 minutes with gentle shaking. After 20 minutes, the dye solution was removed and the wells were washed four times with 1.0 mL distilled water, replacing the water at each 5 minutes interval. The specimens were then air dried, and images were taken. Mineralized areas appear red in color.

#### 2.6. In vivo Rat model studies

Eight male Wistar rats (*Rattus norvegicus*) each weighing 200-250 g were obtained from the Animal house, PSG Institute of Medical Sciences and Research, Coimbatore. The surgical procedure in the rats was approved by the Institutional Animal Ethics Committee, PSG Institute for Medical Sciences & Research, Registration No. 158/PO/ReBi/SL/99/ CPCSEA. The rats were randomly divided into two groups, each containing two rats as given in Table 1. Two rats per cage were housed in a temperature-controlled facility.

**Table 1: Biocompatibility test by subcutaneous implantation of the scaffold in rats**

Period/ scaffold material	Polyamide (PA 12)	PA/HA (90:10) composite
7 weeks	2 rats	2 rats
One year	2 rats	2 rats

#### 2.7. Rat Surgical Procedure

Non-immuno compromised eight male Wistar rats were used for this study. Intraperitoneal injections of Aneket® Ketamine (30 mg/kg) and Astra Zeneca® 2% xylocaine (13 mg/kg) were administered to anesthetize the animals (Figure 2a). The lateral aspect of the abdomen was shaved under aseptic precaution. Using a sterile surgical blade no. 15, an incision of about 3 cm was made (Figure 2b). Skin and subcutaneous tissue was dissected (Figure 2c) and the autoclaved scaffold of dimensions 0.9 mm diameter x 0.4 mm thickness was implanted in the subcutaneous plane (Figure 2d), as given in table 1. Upon implantation of the scaffold in the subcutaneous pouch, the skin was sutured using an Ethicon (5-0) Non-absorbable surgical suture NW 3316 (Jhonson & Jhonson) (Figure 2e). After four days the sutures were found to be eaten off by the rats exposing the scaffolds to outside. The closure was then made using the Glue, N-butyl-2-cyanoacrylate. The animals were fed with rat feed pellets, and the cages were changed every fortnight. Rat surgical procedure was performed according to Subramanian *et al* [12].

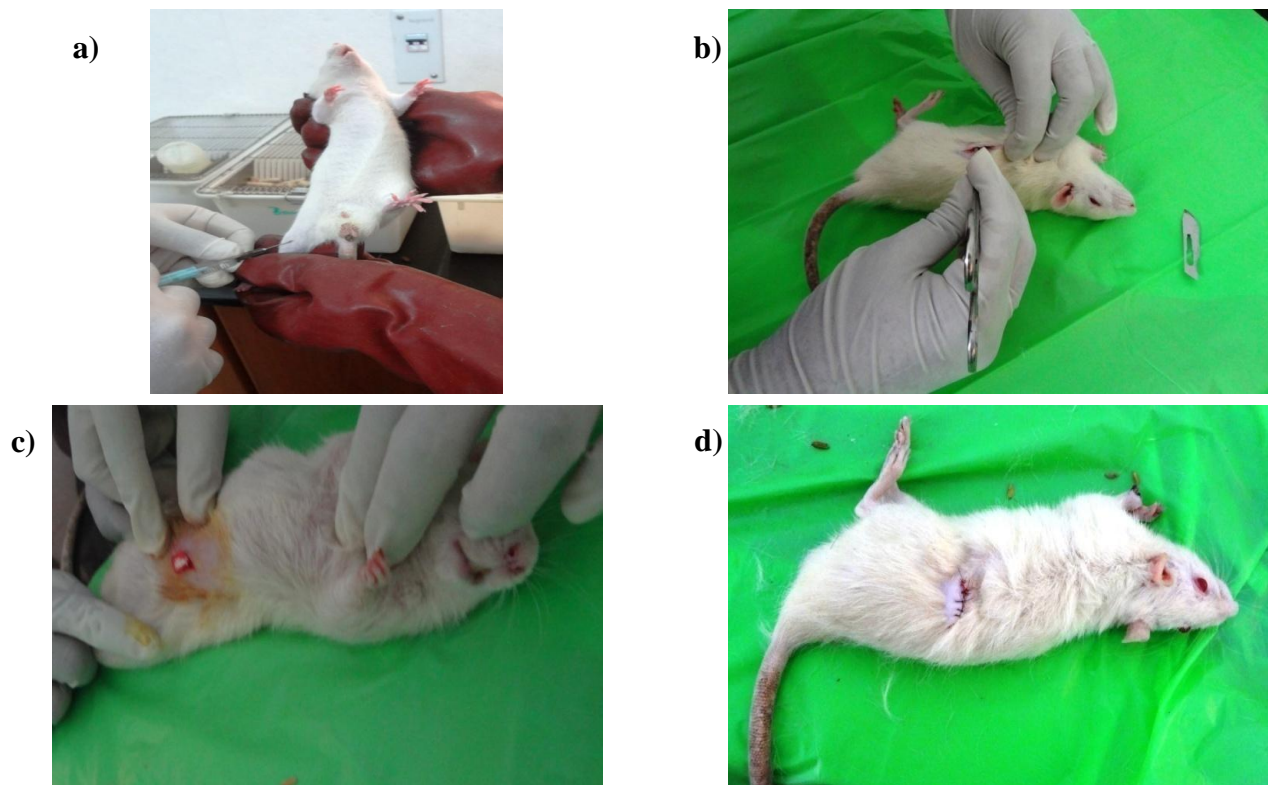


**Figure 2. Rat surgical procedure. (a)administration of general anesthesia; (b) creating a subcutaneous pouch; (c)implanting the autoclaved scaffold; (d)sutured using Ethilon 5-0**

### 2.8. Pathological testing

Post-implantation of the scaffold in the rat model, four rats (two in each group) after 7 weeks, and remaining four rats after one year were euthanized with over dose of diethyl ether. Using the previous scar site, incision was made and the scaffold along with the surrounding tissue was removed. The tissues were stored separately in 10% formalin for histopathological analysis.

### 2.9. Hematoxylin & eosin staining

The samples, with soft tissue cleaned, were stored in 10% formalin for 10 days. The samples were then rinsed in tap water, followed by fixing and dehydration in successive alcohol concentration. The samples were then cleared with xylene and embedded in paraffin wax. After hardening, the sample were cut into 4  $\mu\text{m}$  sections perpendicular to the implants, under cooling water with microtome (Leica RM2255, Germany). The sections were glued onto a plastic support and finally stained with Harris Hematoxylin and Eosin.

## 3. Results and Discussion

Increasing trauma and injuries in day-to-day life demands orthopedic scaffolds with desirable and reproducible design, adequate strength and biocompatibility. Rapid prototyping is one such fabrication technique that facilitates development of customized scaffolds rather than standardized scaffolds, in a short time.

Advantages of custom-made scaffolds of satisfactory size matching the defect area could easily be implanted at the defect site. Besides reducing the time for surgery, custom-made scaffold contributes to the rapid healing of the defects [6]. Selective Laser Sintering uses a high temperature of around 1100°C for fabricating the components. However, the chemical composition of HA and PA were known to remain unmodified even at higher temperatures. Hence, variation in the scaffold properties due to the sintering stays ineffective.

Pores in the bone scaffold aids cellular infiltration and also facilitate the exchange of nutrients and wastes across the bone. The scaffold material becomes more desirable if it supports/enhances cell attachment, proliferation and calcium mineralization in addition to possessing adequate mechanical properties. HA/PA66 composite developed with 75-85% porosity and 500 micron pores yielded the compression strength of 10-20 MPa [14]. Bone screws fabricated using PA/HA without pores yielded bending strength of 200- 300MPa [11]. Porosity is directly proportional to the biological functions of the scaffold, and inversely proportional to the mechanical strength of the scaffold. Hence, fine tailoring of the porosity and pore size without compromising the mechanical property of the scaffold is crucial. The HA/PA12 composite scaffold used in the present study was fabricated with 70% porosity and 800 micron pores using Selective Laser Sintering, discussed

elsewhere [5], yielded a mechanical strength of 25 MPa, which was identified to be adequate to support a person weighing 75 kg.

**3.1 In vitro tests**

From the MTT assay result shown in Figure 3, it can be observed that there is a gradual increase in the cellular proliferation from day 1 to day 5 in all the scaffold types tested including the control. Incorporation of HA in

the composite facilitated better cell attachment and proliferation compared to the polyamide as seen on day 1 and day 5, which could be due to the bioactive nature of the HA. However, it can also be observed that there is no significant difference between the PA/HA (95:5) and PA/HA (90:10) as the percentage increase in minimal. A similar trend was reported by Tang *et al* [13].

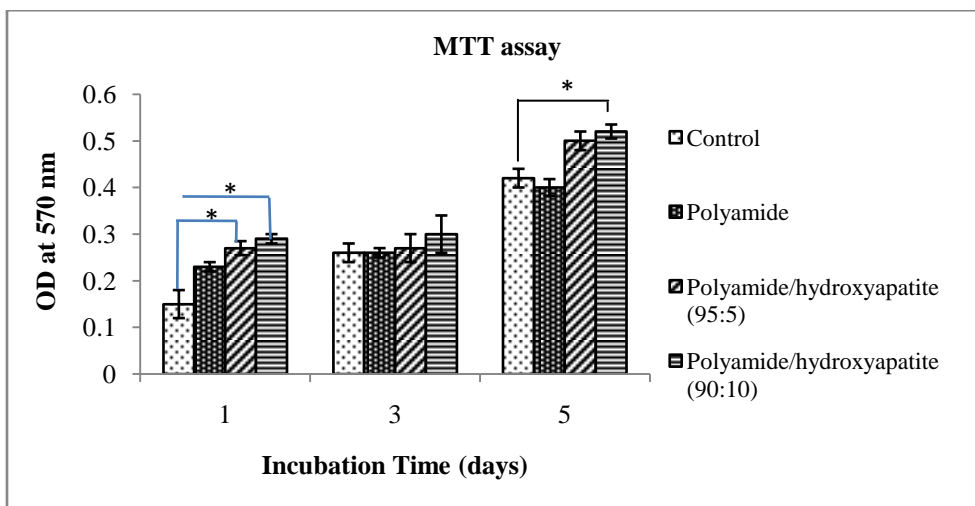


**Figure 3: MTT assay results for MG 63 cells cultured on the scaffolds made of polyamide and various compositions of polyamide/Hydroxyapatite**

ALP is an early differentiation marker for the osteoblasts. A general increase in the ALP activity is observed from day 4 through day 7 in all the scaffolds tested (Figure 4). ALP level in PA/HA (90:10) was

observed to be lower than the control on day 4. However on day 10, the ALP levels of the cells cultured on the PA/HA (90:10) scaffolds were found to be on par with that of the control (cells cultured without scaffold).

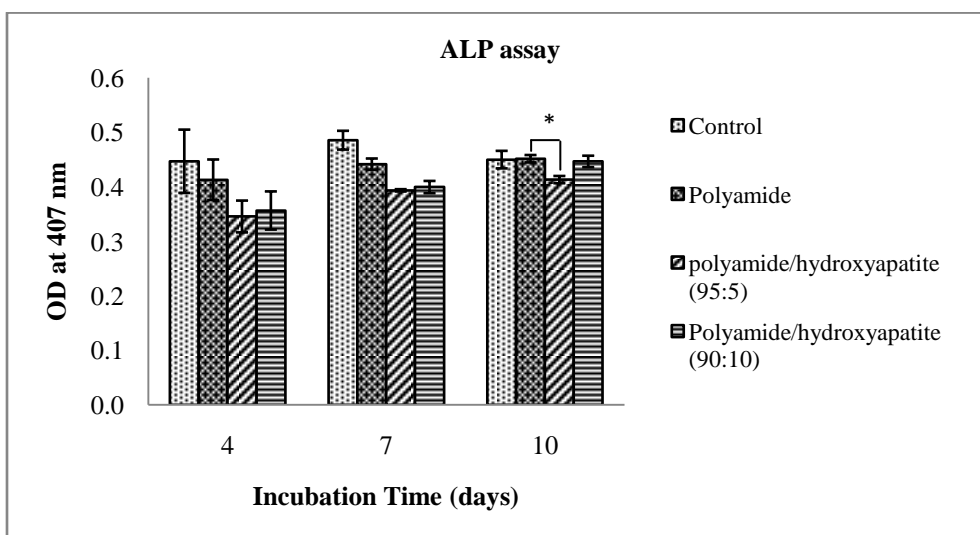


**Figure 4: ALP assay results of MG 63 cells cultured on the scaffolds made of polyamide and different compositions of polyamide/hydroxyapatite**

Alizarin Red S staining results (Figure 5) shows that the polyamide scaffolds were stained less intense than the scaffolds containing HA. These results suggest that though the polyamide was found to be non-cytotoxic and

supporting ALP activity, it lacked the property to support calcium mineralization, which is the desirable criterion for a material to act as a bone scaffold.

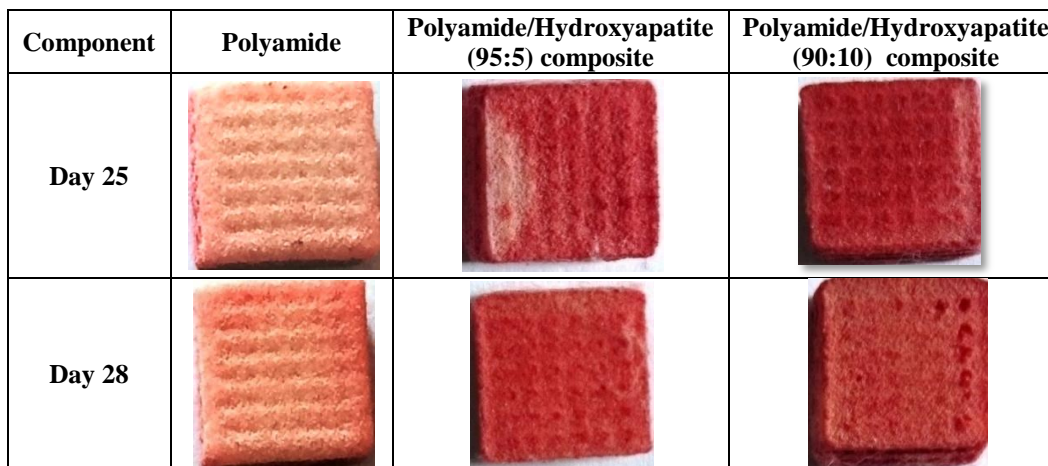
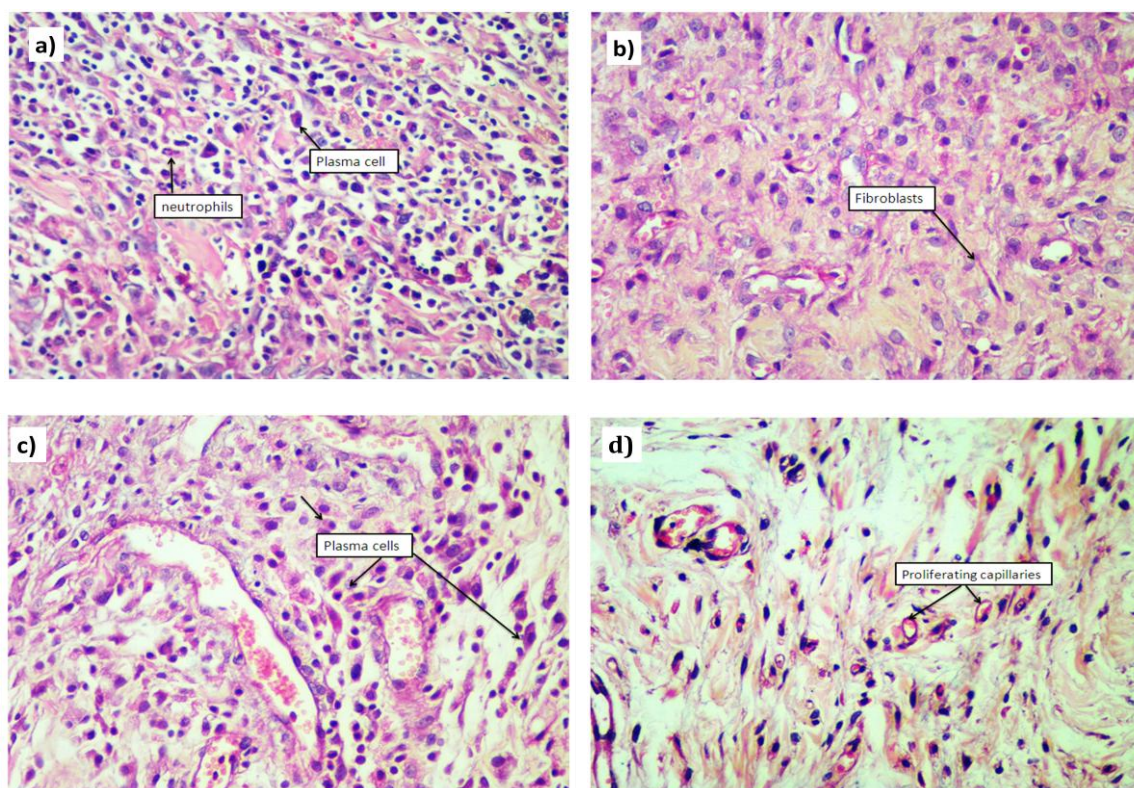


Figure 5: Images of PA/HA (90:10), PA/HA (95:5) and polyamide scaffolds stained with Alizarin red S stain to identify the mineralized regions

### 3.2 In vivo study

There was significant difference in the *in vitro* assays observed between PA and PA/HA composite. However, the difference observed between PA/HA (95:5) and PA/HA (90:10) *in vitro* is minimal, as the percentage variation is lesser. Hence, PA and PA/HA (90:10) scaffolds were implanted subcutaneously in the rat models to analyze their performance *in vivo*. Immunological responses were observed after seven weeks and one year post-implantation in the rat models. Scaffold samples implanted in the rat models were stained with H&E after 7 weeks of implantation. Rat implanted with polyamide showed inflammatory response, whilst the H&E staining results of

PA/HA (90:10) composite suggests that there is no inflammatory response, and the tissues were in the process of healing (Figure 6). Figure 6a and b are replicates for PA scaffold and, 6c and d are the replicates for the PA/HA (90:10) scaffold seven weeks post-implantation in rat. H&E staining of polyamide scaffold (Figure 6a and b) shows plasma cells, neutrophils, fibroblasts and scattered inflammatory infiltrate, while staining of polyamide/hydroxyapatite (90:10) scaffold. Figure 6c and 6d shows fibroblasts, scattered macrophages, plasma cells and occasional neutrophils. Proliferating vascular channels are also seen.



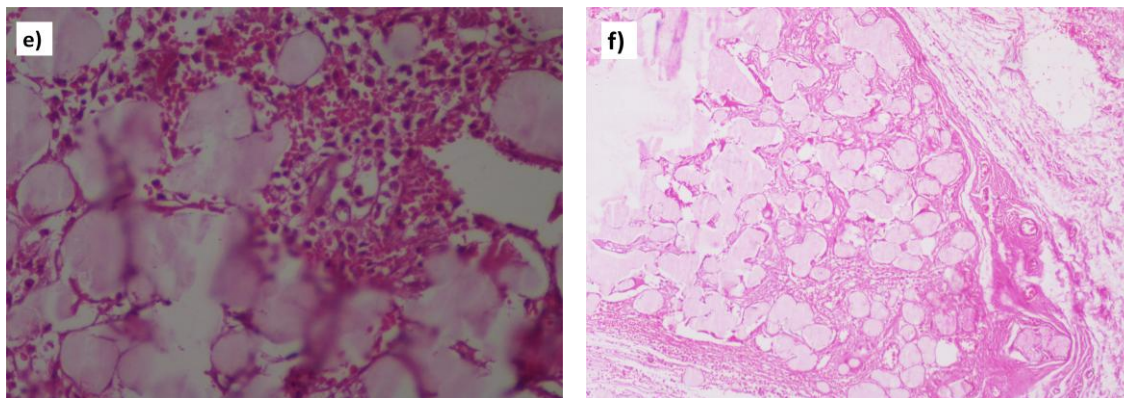


**Figure 6: Representative images of Hematoxylin & eosin staining of polyamide (a and b), and PA/HA(90:10) (c and d) scaffolds after 7 weeks of subcutaneous implantation in rats. And Hematoxylin & eosin staining of polyamide (e), and PA/HA(90:10) (f) scaffolds after one year of subcutaneous implantation in rats.**

During this course of one year observation post-implantation, of four rats (two with PA and two with PA/HA), a rat with polyamide scaffold was deceased on the 11<sup>th</sup> month post-implantation due to its age. Meanwhile complete scaffold disintegration was observed in the rat with PA/HA (90:10) scaffold at the end of one year. Consequently, one in each scaffold type were obtained and subjected to pathological analysis, the images of which are presented in Figure 6e & f.

H&E staining of one year old PA scaffold section (Figure 6e) shows fibroblastic reaction, collagenisation and scant inflammatory infiltrate, while PA/HA (90:10) composite scaffold section (Figure 6f) shows sclerosis, mixed inflammatory infiltrate and focal hyalinization. These results suggest that both the scaffold types were biocompatible.

Post-implantation, follow-up for longer durations of one-year was carried out to identify the scaffold failures due to infection, failure of osseointegration or implant loss by mechanical loading [6]. Staffa *et al* suggests a two year follow-up of porous HA cranial prosthesis as per the protocol of Neurosurgicals. This would facilitate the monitoring of osseointegration. A perfect fit between the implant and the bone allows in-growth of capillaries, perivascular mesenchymal tissue and osteoprogenitor cells from the living bone into the graft. This is crucial to validate the success of the bone implant [10]. Xiong *et al* performed a longer follow-up of rabbit tibial defects fixed with PA/HA composite for internal fixation loosening and joint collapse till 5.3 years [14]. In our study, analysis after one year of implantation was carried out. However, neither any infection nor any inflammation was observed.

Burnett *et al* assessed the safety of using Polyamide and reported to be used in cosmetics and personal care products. And the acute oral LD<sub>50</sub> for polyamide 12 was reported to be 1g per kg of body weight in rat, mice, guinea pigs and rabbits [2]. Recently,

Polyamide is used with nano-hydroxyapatite for developing bone screws [11] and vertebral plates [14]. PA/HA composite has entered the clinical trials for testing in the proximal and distal regions of femur, tibia and humerus in humans [14].

#### 4. Conclusion

3D porous PA and PA/HA scaffolds were tested *in vitro* and *in vivo*. *In vitro* tests such as MTT assay, ALP assay and Alizarin Red S staining carried out using MG 63 cell line reveals that all the three types of scaffolds (PA, PA/HA (95:5) and PA/HA (90:10)) were non-cytotoxic. However, PA/HA (90:10) outperformed the three scaffold types tested. Hence, pure PA and PA/HA (90:10) scaffolds were implanted subcutaneously in the rat models. Pathological tests of 7 week old scaffolds showed that polyamide scaffold showed presence of inflammatory cells, whilst the PA/HA (90:10) composite scaffold showed presence of proliferating capillaries and were in the process of healing. However, pathological testing of scaffolds one year post-implantation showed that both scaffold types were biocompatible and neither showed immune rejection nor infection. The PA/HA (90:10) composite having performed consistently better under *in vitro* and *in vivo* conditions, we conclude that the above composite could more likely be used in orthopedic applications.

#### Acknowledgment

The authors acknowledge the Department of Science and Technology, Government of India - Grant No. SR/S3/MERC-0040 (2012) for providing the fund to carry out this research work. The authors also thank the PSG TIFAC-CORE and PSG Animal House facility for their support.

#### Conflict of interest

Authors declare no conflict of interest.

## References

- [1]. Bougherara H, Bureau M N, Yahia L. Bone remodeling in new biomimetic polymer-composite hip stem. *J Biomed Mater Res Part A*. 2010; 92(1):164-174.
- [2]. Burnett C, Heldreth B, Bergfeld W F, Belsito D V, Hill R A, Klaassen C D, Liebler D C, Marks Jr J G, Shank R C, Slaga T J, Snyder P W, Andersen F A. Safety Assessment of Nylon as Used in Cosmetics. *Int. J. Toxicol*. 2014; 33(4) 47S-60S.
- [3]. Gregory C A, Gunn W G, Peister A, Prockop D J. An Alizarin red-based assay of mineralization by adherent cells in culture: comparison with cetylpyridinium chloride extraction. *Anal. Biochem*. 2004; 329(1):77-84.
- [4]. Henkel J, Woodruff M A, Epari D R, Steck R, Glatt V, Dickinson I C, Choong P F M, Schuetz M A, Hutmacher D W. Bone Regeneration Based on Tissue Engineering Conceptions – A 21<sup>st</sup> Century Perspective. *Bone Res*. 2013; 1(3): 216-248.
- [5]. Kumaresan T, Gandhinathan R, Ramu M, Ananthasubramanian M, Banu Pradheepa K. Design, analysis and fabrication of polyamide/ hydroxyapatite porous structured scaffold using selective laser sintering method for bio-medical Applications. *J. Mech. Sci. Technol*. 2016; 30 (11):5305-5312.
- [6]. Mangano F, Macchi A, Shibli JA, Luongo G, Lezzi G, P A, Caprioglio A, Mangano C. Maxillary Ridge Augmentation with Custom-made CAD/CAM scaffolds. A 1-Year Prospective Study on 10 Patients. *J. Oral Implantol*. 2014; 40(5): 561-569.
- [7]. Qiao B, Li Lidong, Zhu Q, Guo S, Qi X, Li W, Wu J, Liu Y, Jiang D. Bone plate composed of a ternary nano-hydroxyapatite/polyamide 66/glass fiber composite: biomechanical properties and biocompatibility. *Int. J. Nanomedicine*. 2014; 9: 1423-1432.
- [8]. Qu Y, Wang P, Man Y, Zuo Y, Li J. Preliminary biocompatible evaluation of nano-hydroxyapatite/polyamide 66 composite porous membrane. *Int. J. Nanomedicine*. 2010; 2: 429-435.
- [9]. Sneha M, Sundaram N M. Preparation and characterization of an iron-oxide-hydroxyapatite nanocomposite for potential bone cancer therapy. *Int. J. Nanomedicine* 2015; 10 (1): 99-106.
- [10]. Staffa G, Barbanera A, Faiola A, Fricia M, Limoni P, Mottaran R, Zanotti B, Stefini R. Custom made bioceramic implants in complex and large cranial reconstruction: A two-year follow-up. *J. Cranio Maxillo Fac. Surg*. 2012; 40: 65-70.
- [11]. Su B, Peng X, Jiang D, Wu J, Qiao B, Li W, Qi X. In Vitro and In Vivo Evaluations of Nano-Hydroxyapatite/Polyamide 66/Glass Fibre (n-HA/PA66/GF) as a Novel Bioactive Bone Screw. *PLoS ONE* 2013; 8(7): e68342.
- [12]. Subramanian A, Krishnan U, Sethuraman S. In vivo Biocompatibility of PLGA-polyhexylthiophene Nanofiber Scaffolds in Rat Model. *Biomed Research International* 2013; Article ID 390518.
- [13]. Tang Y, Wu C, Wu Z, Hu L, Zhang W, Zhao K. Fabrication of in vitro biological properties of piezoelectric bioceramics for bone regeneration. *Sci. Rep*. 2017; 7, 43360.
- [14]. Xiong Y, Ren C, Zhang B, Yang H, Lang Y, Min Y, Zhang W, Pei F, Yan Y, Li H, Mo A, Tu C, Duan H. Analyzing the Behaviour of a porous nano-hydroxyapatite/polyamide 66 (n-HA/PA66) composite for healing of Bone Defects. *Int. J. Nanomedicine* 2014; 9: 485-494.
- [15]. Yao M, Fu M, Liu H, wang x, Sheng X, Gao J. Fabrication and characterization of drug-loaded nano-hydroxyapatite/polyamide 66 scaffolds modified with carbon nanotubes and silk fibroin. *Int. J. Nanomedicine* 2016; 11: 6181-6194.
- [16]. You F, Li Y, Zou Q, Zuo Y, Lu M, Chen X, Li L. Fabrication and osteogenesis of a Porous nanohydroxyapatite/polyamide scaffold with an Anisotropic Architecture. *ACS Biomat. Sci. Eng*. 2015; 1(5): 825-833.
- [17]. Zhou S, Zhang I, Wang Y, Zuo Y, Gao S, Li Y. Fabrication of hydroxyapatite/Ethylene vinyl Acetate/ Polyamide 66 Composite Scaffolds by Injection-Moulding Method. *Polym. Plast. Technol. Eng*. 2011 Jul 12; 50(10): 1047-1054.
- [18]. [http://ec.europa.eu/eurostat/statistics-explained/index.php/Accidents\\_at\\_work\\_statistics#Analysis\\_by\\_type\\_of\\_injury](http://ec.europa.eu/eurostat/statistics-explained/index.php/Accidents_at_work_statistics#Analysis_by_type_of_injury)
- [19]. <https://www.xpneumatic.com/difference-between-pa6-pa11-and-pa12/>
- [20]. [http://webhotel2.tut.fi/projects/caeds/tekstit/plastics/plastics\\_POLYAMIDES.pdf](http://webhotel2.tut.fi/projects/caeds/tekstit/plastics/plastics_POLYAMIDES.pdf)